THE JOURNAL OF BIOLOGICAL CHEMISTRY VOL. 282, NO. 1, pp. 58–64, January 5, 2007

A Novel Neutrophil Elastase Inhibitor Prevents Elastase Activation and Surface Cleavage of the Epithelial Sodium Channel Expressed in *Xenopus laevis* Oocytes*

Received for publication, May 30, 2006, and in revised form, October 17, 2006 Published, JBC Papers in Press, November 7, 2006, DOI 10.1074/jbc.M605125200

Michael Harris[‡], Dmitri Firsov[‡], Grégoire Vuagniaux[§], M. Jackson Stutts[¶], and Bernard C. Rossier[‡1]

From the [‡]Département de Pharmacologie et de Toxicologie, Université de Lausanne, CH-1005 Lausanne, Switzerland, [§]Debiopharm SA, CH-1000 Lausanne, Switzerland, and [¶]University of North Carolina, Chapel Hill, North Carolina 27599-7248

The amiloride-sensitive epithelial sodium channel (ENaC) constitutes a limiting step in sodium reabsorption across distal airway epithelium and controlling mucociliary clearance. ENaC is activated by serine proteases secreted in the extracellular milieu. In cystic fibrosis lungs, high concentrations of secreted neutrophil elastase (NE) are observed. hNE could activate ENaC and contribute to further decreased mucociliary clearance. The aims of this study were (i) to test the ability of an engineered human neutrophil elastase inhibitor (EPI-hNE4) to specifically inhibit the elastase activation of ENaC-mediated amiloride-sensitive currents (I_{Na}) and (ii) to examine the effect of elastase on cell surface expression of ENaC and its cleavage pattern (exogenous proteolysis). Oocytes were exposed to hNE (10–100 μg/ml) and/or trypsin (10 μg/ml) for 2–5 min in the presence or absence of EPI-hNE4 (0.7 μM). hNE activated I_{Na} 3.6-fold ($p < 0.001$) relative to non-treated hENaC-injected oocytes. EPI-hNE4 fully inhibited hNE-activated I_{Na} but had no effect on trypsin- or prostasin-activated I_{Na}. The co-activation of I_{Na} by hNE and trypsin was not additive. Biotinylation experiments revealed that cell surface γ ENaC (but not α or β ENaC) exposed to hNE for 2 min was cleaved (as a 67-kDa fragment) and correlated with increased I_{Na}. The elastase-induced exogenous proteolysis pattern is distinct from the endogenous proteolysis pattern induced upon preferential assembly, suggesting a causal relationship between γ ENaC cleavage and ENaC activation, taking place at the plasma membrane.

The highly sodium-selective epithelial sodium channel (ENaC)[2] is composed of three homologous subunits (α, β, γ) and is expressed in several ion-transporting epithelia, including the kidney, colon, and lung (1). The physiological importance of ENaC in the lung was recognized when α ENaC knock-out mice were shown to die prematurely because of defective lung liquid clearance (2), indicating ENaC as a major driving force for fluid reabsorption from the alveolar space at the time of birth. Active transepithelial sodium transport by surface airway epithelia provides a major driving force for the control of airway surface liquid and periciliar liquid (PCL), highly critical for mucociliary clearance (3, 4). ENaC, located at the apical membrane of the surface airways epithelium (SAE), constitutes a limiting step for sodium absorption by SAE, as shown by human genetic diseases (5). Thus, loss of function of ENaC, as observed in pseudohypoaldosteronism, leads to a 2–3-fold *increase* in mucociliary clearance (6). By contrast, increased ENaC activity, secondary to a loss of function of the cystic fibrosis transmembrane regulator, is observed in cystic fibrosis (CF) patients. CF is a disease that is characterized by mutation of the cystic fibrosis transmembrane regulator gene (7). The cystic fibrosis transmembrane regulator is responsible for Cl^--driven fluid secretion in upper and lower airways and inhibits antagonistic fluid absorption through ENaC (8, 9). CF patients thus experience a severe *decrease* in mucociliary clearance (10). Mall *et al.* (11) have recently established that increased ENaC expression and activity in airways of transgenic mice may cause *per se* a "cystic fibrosis-like lung disease" characterized by decreased mucociliary clearance and tissue inflammation even in the absence of microbial infection. Together, these findings suggest that over-activity of ENaC contributes significantly to the CF phenotype. Thus, ENaC becomes a valid drug target for treating CF patients.

Numerous studies have shown that several serine proteases are capable of increasing ENaC-mediated I_{Na} in multiple cell types (12), including the *in vitro* and *in vivo* rodent lung (13–15). The activation of ENaC by serine proteases may be a direct consequence of proteolytic cleavage (16) by a dramatic change in its open probability (P_o) (17). Because over-activity of ENaC is capable of inducing a CF-like phenotype, proteolytic activation of ENaC could be detrimental to CF patients.

The serine protease neutrophil elastase (hNE) has been shown to reach concentrations >200 μg/ml in the lungs of patients with CF (21) and to overcome antiprotease activity (19), whereas healthy subjects have undetectable levels of hNE. The hNE in the lungs of patients with CF is known to cause cellular damage, production of the pro-inflammatory cytokine interleukin 8, and increased neutrophil influx (20) (21, 22). If hNE is also capable of activating ENaC, it would thereby exacerbate the CF phenotype and actions taken to reduce this activation could be beneficial to CF patients. Recently, Caldwell

* This work was supported by grants from the Novartis Foundation in 2003 (to B. C. R.) and the Swiss National Foundation (3100-061966 (to B. C. R.) and 3100A0-105592 (to D. F.)). The costs of publication of this article were defrayed in part by the payment of page charges. This article must therefore be hereby marked "*advertisement*" in accordance with 18 U.S.C. Section 1734 solely to indicate this fact.

[1] To whom correspondence should be addressed: Dépt. de Pharmacologie et de Toxicologie, Université de Lausanne, 27, Rue du Bugnon, CH-1005 Lausanne, Switzerland. Tel.: 4121-692-5351; Fax: 4121-692-5355; E-mail: Bernard.Rossier@unil.ch.

[2] The abbreviations used are: ENaC, epithelial sodium channel; PCL, periciliar liquid; NE, neutrophil elastase; MBS, modified Barth solution; CAP, channel-activating protease.

et al. (23) have shown that hNE is capable of stimulating I_{Na} in a human bronchiole cell line and that an elastase inhibitor can prevent elastase-mediated stimulation.

Elastase inhibitor therapy is currently being developed to treat CF and chronic obstructive pulmonary disease by preventing hNE-induced lesions in the pulmonary epithelium. In this study, we have examined the effectiveness of one of these compounds, EPI-hNE4, an engineered hNE inhibitor that was designed to be a specific, high affinity drug, resistant to oxidative and proteolytic inactivation.

We have hypothesized that hNE can cleave cell surface-expressed ENaC, which results in channel activation, and that EPI-hNE4 can prevent this cleavage/activation. To identify whether ENaC was being directly cleaved by hNE, oocytes were analyzed for increased ENaC-mediated I_{Na} and for proteolytic cleavage of cell surface proteins. Here, we present data indicating that elastase is capable of activating ENaC, possibly by cleaving cell surface-expressed γ ENaC and that this effect can be blocked by the elastase-specific inhibitor EPI-hNE4. The elastase-induced cleavage (exogenous proteolysis) is distinct from the cleavage pattern observed upon preferential assembly of α, β, and γ ENaC subunits by oocyte proteases (endogenous proteolysis), suggesting a causal relationship between cleavage and ENaC activation.

EXPERIMENTAL PROCEDURES

cRNAs—Complementary RNAs of human or rat $\alpha\beta\gamma$ ENaC subunits and human prostasin were synthesized *in vitro*, using SP6 and T7 polymerase. C terminus V5 epitope-tagged α, β, and γ ENaC subunits were created by PCR amplification. For each subunit, two primers were synthesized. The forward primer contains the SpeI site and the start codon of the ENaC gene; the reverse primer contains the NotI site, the coding sequence for V5, and the C-terminal sequence of the ENaC gene. PCR products were purified and cloned into the SpeI/NotI sites of pSDE vector.

Antibodies—Monoclonal anti-V5 antibody was obtained from Invitrogen and used according to the manufacturer's instruction. The actin antibody was from Sigma.

Expression of ENaC and Human Prostasin cRNA in Xenopus oocytes—The cRNAs were injected into *Xenopus* oocytes (3.3 ng of each subunit and 3.3 ng of human CAP-1 (prostasin) = 13.2 ng of total cRNA/oocyte), and injected oocytes were kept in modified Barth solution (MBS) containing 88 mM NaCl, 1 mM KCl, 2.4 mM $NaHCO_3$, 0.8 mM $MgSO_4$, 0.3 mM $Ca(NO_3)_2$, 0.4 mM $CaCl_2$, 10 mM Hepes-NaOH, pH 7.2. Electrophysiological measurements and cell surface biotinylation were performed 24 h after injection. Amiloride-sensitive Na^+ current (I_{Na}) was recorded using the two-electrode voltage clamp and was defined as the difference between Na^+ current obtained in the presence (5 μM) and in the absence of amiloride.

Incubation of Xenopus oocytes with Proteases and Inhibitors—ENaC-injected oocytes were incubated for 2 min at room temperature in MBS solution containing proteases and/or inhibitors. hNE from human neutrophils (Serva Electrophoresis) was used at a concentration of 10–100 μg/ml, trypsin (Sigma) was used at a concentration of 10 μg/ml, engineered human elastase inhibitor (Debiopharm SA) was used at a concentration of 4.4 μg/ml, and aprotinin was used overnight at a concentration of 100 μg/ml. At the end of the incubation, elastase inhibitors were added to all samples before biotinylation.

Biotinylation of ENaC Subunits on the Cell Surface—Biotinylation was performed in 40-well plates, using 50 oocytes/experimental condition as described (24). All biotinylation steps were performed at 4 °C. After incubation in MBS solution for 30 min at 4 °C, the oocytes were washed three times with MBS. After the last wash, the MBS solution was removed and replaced by a biotinylation buffer containing 10 mM triethanolamine, 150 mM NaCl, 2 mM $CaCl_2$, 1 mg/ml EZ-link sulfo-NHS-SS-Biotin (Pierce), pH 9.5. The incubation lasted 15 min with gentle agitation. The biotinylation reaction was stopped by washing the oocytes two times with Quench buffer containing 192 mM glycine, 25 mM Tris-Cl, pH 7.5, added to MBS solution. After the second wash, oocytes were incubated for 5 min in the Quench buffer with gentle agitation. Oocytes were then washed two times with MBS solution and lysed by repeated pipetting with Pasteur pipettes in lysis buffer containing 1% Triton X-100, 500 mM NaCl, 5 mM EDTA, 50 mM Tris-Cl, 5 μg/ml each of leupeptin, antipain, and pepstatin, 10 μg/ml aprotinin, and 4.4 μg/ml EPI-hNE4 (20 μl/oocyte). The lysates were vortexed for 30 s and centrifuged for 10 min at ~10,000 × *g*. Supernatants were transferred to the new 1.5-ml Eppendorf tubes containing 50 μl of immunopure immobilized streptavidin beads (Pierce) washed with lysis buffer. After overnight incubation at 4 °C with agitation, the tubes were centrifuged for 1 min at 5,000 rpm. Supernatant was removed, and beads were washed three times with lysis buffer. 35 μl of 2× SDS-PAGE sample buffer was added to the beads. All samples were heated for 5 min at 95 °C before loading on the 8–15% SDS-PAGE.

RESULTS

The endogenous processing of ENaC in the *Xenopus* oocyte expression system is significant and specific for each subunit. Hughey *et al.* (16) have implicated furin in ENaC proteolytic processing. It is not known if other enzymes are involved, and it is not clear whether this processing is related to the activation of ENaC at the cell surface. The study of exogenous secreted serine proteases (trypsin, elastase) could help in understanding whether ENaC cleavage is required for activation or not. We coupled the use of hNE with a highly specific inhibitor to study the relationship between cleavage of ENaC at the cell surface and the sodium transport response.

Engineered Elastase Inhibitor EPI-hNE4 Specifically Inhibits Human hNE, and Not Trypsin, Stimulation of hENaC—To determine whether EPI-hNE4 was capable of inhibiting hNE-mediated stimulation of hENaC, we used the *Xenopus* oocyte expression system to overexpress hENaC proteins by injecting α, β, and γ hENaC subunit cRNAs. *Xenopus* oocytes injected with hENaC were exposed to hNE for 2 min, and I_{Na} was measured using the two-electrode voltage clamp system. Exposure of the *Xenopus* oocytes to hNE in MBS solution resulted in a >3.5-fold increase in I_{Na} over untreated oocytes (Fig. 1, *lane 2 versus lane 1*). This stimulation of hENaC (*lane 2*) was significantly inhibited in oocytes exposed to hNE in the presence of the elastase inhibitor EPI-hNE4 (*lane 3*), suggesting that the catalytic activity of hNE is involved in the activation of ENaC. Trypsin

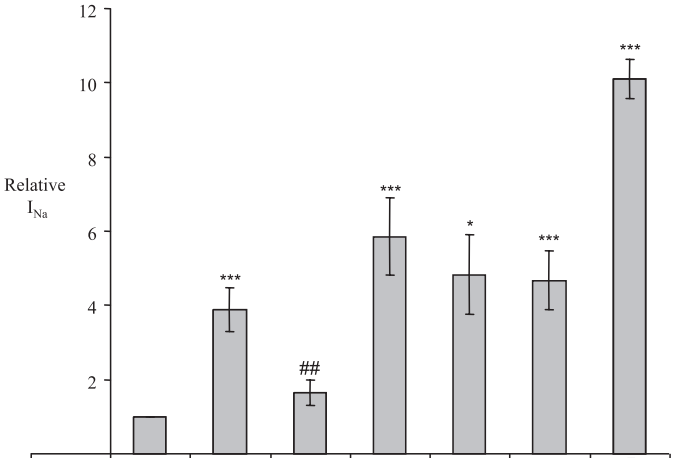

Lane	1	2	3	4	5	6	7
Elastase	-	+	+	-	-	+	10x [ENaC]
Trypsin	-	-	-	+	+	+	
EPI-hNE4	-	-	+	-	+	-	

FIGURE 1. **Engineered elastase inhibitor EPI-hNE4 specifically inhibits hNE, and not trypsin, stimulation of hENaC.** Oocytes were injected with $\alpha\beta\gamma$ hENaC cRNAs 24 h before experimental analyses. Oocytes were exposed to hNE (100 μg/ml), trypsin (10 μg/ml), and an hNE inhibitor EPI-hNE4 (44 μg/ml) for 2 min at room temperature before I_{Na} was measured by voltage clamp technique. Shown is relative (relative to untreated ENaC-injected oocytes with I_{Na} of 2.7 $\pm$ 0.6 μA) mean $\pm$ S.E. of three independent experiments performed with six oocytes/experimental condition). ***, $p < 0.001$ *versus lane 1*; *, $p < 0.05$ *versus lane 1*; ##, $p < 0.01$ *versus lane 2* by Student's *t* test.

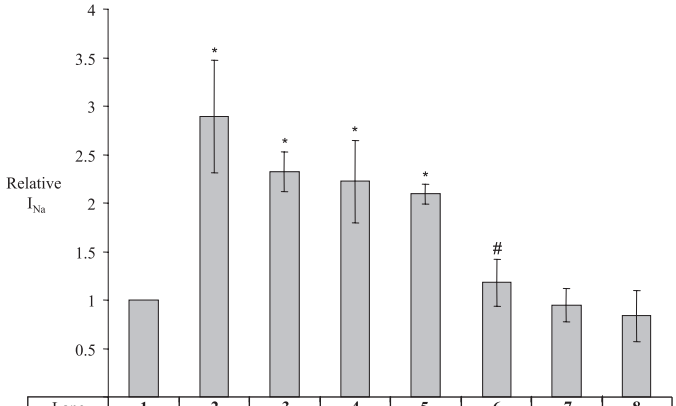

Lane	1	2	3	4	5	6	7	8
hCAP1	-	+	+	+	+	+	-	-
EPI-hNE4	-	-	5pg/ml	5ng/ml	5µg/ml	-	5µg/ml	-
Aprotinin	-	-	-	-	-	+	-	+

FIGURE 2. **EPI-hNE4 does not inhibit amiloride-sensitive Na^+ transport induced by co-injected hCAP1.** Co-expression of $\alpha\beta\gamma$ hENaC with hCAP1 caused increased I_{Na} (*lane 2*), which was not inhibited by EPI-hNE4 (*lanes 3–5*, concentration indicated; $p < 0.05$, *lanes 2–5* versus *lane 1* (control)) but was inhibited by 100 μg/ml aprotinin (*lane 6*, #, $p < 0.05$ *versus lane 2*). Shown is relative (relative to untreated ENaC-injected oocytes with I_{Na} of 3.1 $\pm$ 0.8 μA) mean $\pm$ S.E. of four independent experiments performed with five oocytes/experimental condition.

stimulated I_{Na} in hENaC-injected oocytes >5.5-fold over non-treated oocytes (*lane 4*), but EPI-hNE4 did not inhibit trypsin-induced activation of hENaC (*lane 5*), demonstrating the specificity of the inhibitor for elastase. Thus, both hNE and trypsin activate ENaC. To determine whether the activation pathways for these proteases were similar, hENaC-injected oocytes were exposed to trypsin alone (*lane 4*) or to hNE and trypsin together (*lane 6*). Simultaneous exposure to hNE and trypsin resulted in a 5-fold increase in I_{Na} (*lane 6*), but no additive effect was observed (compare *lanes 6 versus 4* and *6 versus 2*). This non-additive stimulation of I_{Na} in hENaC-injected oocytes by hNE and trypsin suggests that each protease can achieve maximum proteolytic stimulation of ENaC, either through proteolytic cleavage of the channel itself or through one of its regulatory proteins. The possibility that the expression system was translationally saturated was ruled out by injecting ten times more ENaC cRNAs, leading to a >10-fold increase in I_{Na} (*lane 7*).

EPI-hNE4 Does Not Inhibit Amiloride-sensitive Na^+ Transport Induced by Co-injected Prostasin—Channel-activating proteases (CAPs) are membrane-bound serine proteases (12) known to be expressed and to regulate ENaC in the lung (13–15). To determine whether EPI-hNE4 was capable of inhibiting exogenously expressed membrane proteases, hENaC-injected oocytes were co-injected with human CAP-1 (prostasin) (Fig. 2), a serine protease known to be expressed in airway epithelia and known to increase amiloride-sensitive I_{Na}. Oocytes co-injected with hCAP-1 and hENaC significantly increased I_{Na} (3-fold) (*lane 2*) over hENaC-injected oocytes (*lane 1*). Increasing concentrations of EPI-hNE4 added at the time of cRNA injection (*lanes 3–5*) were unable to significantly decrease the CAP-1-induced increase in I_{Na}. This further indicated that EPI-hNE4 is specific for hNE and does not affect human CAP-1 (prostasin) activity. As shown previously, the protease inhibitor aprotinin (added at the time of cRNA injection) was able to significantly decrease the prostasin-mediated increase in I_{Na} (*lane 6*), indicating that inhibition of CAP-1-mediated stimulation was effective. EPI-hNE4 had no significant effect on amiloride-sensitive I_{Na} when applied in the absence of hNE (*lane 7*). Aprotinin had no significant effect on basal currents (*lane 8*).

NE Cleaves γ rENaC, but Not α and β rENaC, and Is Specifically Inhibited by EPI-hNE4—Recently, Hughey *et al.* (25) have shown that ENaC is proteolytically processed. It was demonstrated that cell surface-expressed ENaC proteins are cleaved and that cleavage correlated with channel activity. This suggested that intracellular proteolytic cleavage was involved in channel maturation (25). The mechanism of extracellular protease stimulation of ENaC activity has not been identified. We wished to determine whether extracellular stimulation of ENaC by hNE was correlated with direct cleavage of the channel at the cell surface.

Exposure of rENaC-injected *Xenopus* oocytes to hNE increased amiloride-sensitive Na^+ current (I_{Na}) >7.5-fold ($p < 0.001$, $n = 13$) within 2 min. This stimulation of rENaC by hNE was significantly inhibited ($p < 0.001$) when the elastase inhibitor EPI-hNE4 was present in the MBS solution. To determine whether hNE activation was mediated by direct cleavage of the cell surface-expressed protein, cell surface biotinylation was performed. *Xenopus* oocytes injected with rENaC and exposed briefly (2 min) to hNE alone or to hNE and EPI-hNE4 together were biotinylated to separate membrane and intracellular proteins. Biotinylated and non-biotinylated V5-tagged α rENaC coinjected with β and γ rENaC was separated on a 8–15% gradient PAGE, transferred to a nitrocellulose membrane for Western blotting, and probed with V5 antibody (Fig. 3*B*). Control oocytes as well as those exposed to hNE, and hNE4 in the presence of EPI-hNE4 (*lanes 1–3*, respectively), had a major band at 95 kDa as well as 80- and 65-kDa fragments corre-

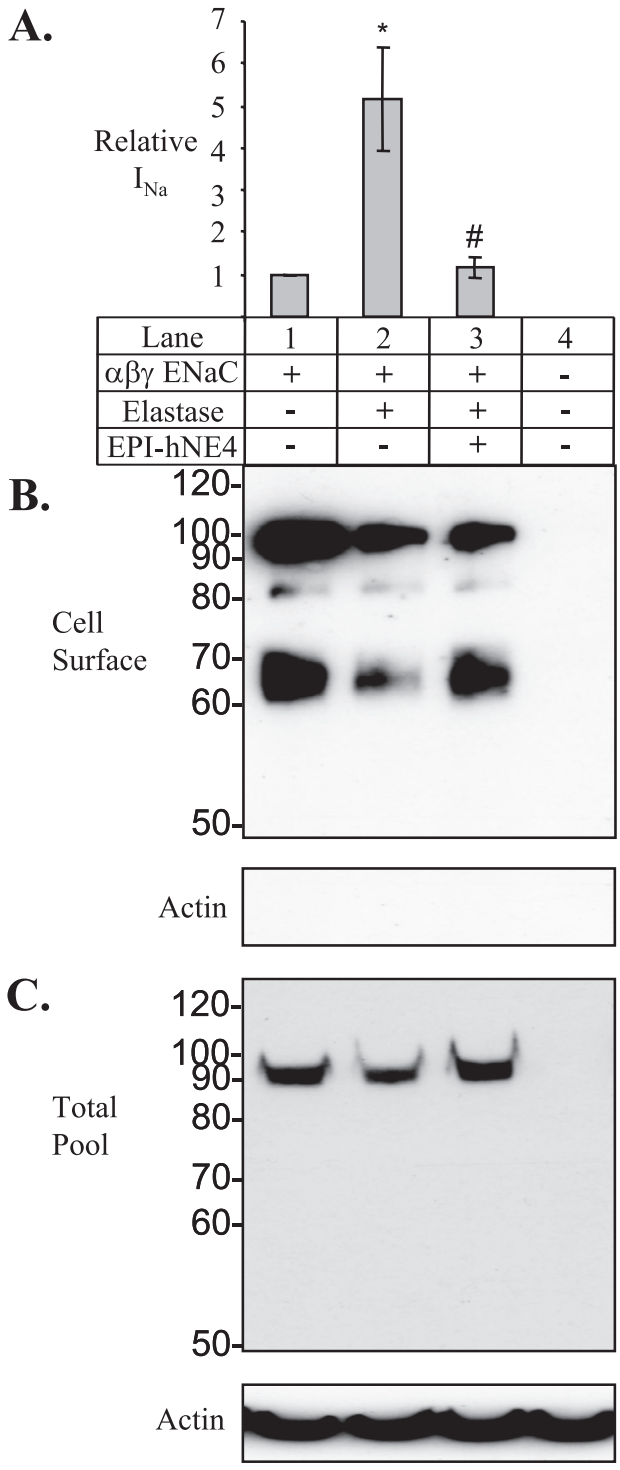

FIGURE 3. **hNE does not cleave cell surface-expressed α ENaC.** Wild-type β and γ rENaC were co-injected with V5-tagged α rENaC in *Xenopus laevis* oocytes. *A*, amiloride-sensitive current was measured in untreated oocytes (3.1 ± 1.3 μA, *lane 1*), oocytes exposed to 10 μg/ml hNE (*lane 2*), 10 μg/ml hNE in the presence of EPI-hNE4 (*lane 3*), and non-injected oocytes (*lane 4*) in five independent experiments. hNE significantly activated ENaC (*, $p < 0.05$), and this activation was inhibited by EPI-hNE4 (#, $p < 0.05$). Cell surface-biotinylated proteins (surface) and non-biotinylated proteins (total pool) were probed with V5 antibody to detect the V5 tag inserted in the C terminus of α ENaC. *B*, biotinylated cell surface proteins. Full-length 95-kDa α ENaC as well as 80- and 65-kDa fragments were expressed at the cell surface in ENaC-injected oocytes (*lanes 1–3*). Treatment with hNE did not produce any additional cleavage products (*lane 2*). *C*, non-biotinylated protein pool. The non-biotinylated protein pool contained full-length 95-kDa α ENaC in ENaC-injected oocytes (*lanes 1–3*). Absence of actin in the biotinylated proteins indicated that no non-biotinylated proteins were labeled. Even quantities of actin in the non-biotinylated proteins indicated even protein loading.

sponding to the full-length α ENaC molecule, and two cleavage products. The non-biotinylated protein pool (Fig. 3*C*) also contained the 95-kDa full-length α ENaC molecule, but not the 80- and 65-kDa fragments (*lanes 1–3*). These products were ENaC specific and not observed in water-injected oocytes (*lane 4*). Absence of actin in the biotinylated cell surface proteins and its presence in the non-biotinylated protein pool confirmed that the biotinylation reaction did not label intracellular proteins. This result indicated that α ENaC was not cleaved by hNE but was cleaved by endogenous proteases. The corresponding amiloride-sensitive I_{Na} currents are shown in *panel A* showing a 5-fold increase of I_{Na} after 2 min of incubation in the presence of elastase, an effect fully inhibited by the inhibitor.

V5-tagged β rENaC coinjected with α and γ ENaC was also Western blotted and probed with V5 antibody. β ENaC was expressed as a single band of 105 kDa at the cell surface (Fig. 4*B*, *lanes 1–3*) as well as in the non-biotinylated protein pool (Fig. 4*C*, *lanes 1–3*) in all ENaC-injected conditions. These products were ENaC specific and not observed in water-injected oocytes (*lane 4*). This result indicated that β ENaC was not cleaved by hNE or by intracellular proteases. The corresponding amiloride-sensitive I_{Na} currents are shown in *panel A* showing a 5-fold increase of I_{Na} after 2 min of incubation in the presence of elastase, an effect fully inhibited by the inhibitor.

V5-tagged γ rENaC coinjected with α and β rENaC was also Western blotted and probed with V5 antibody. Control oocytes as well as those exposed to hNE and hNE4 in the presence of EPI-hNE4 (Fig. 5*B*, *lanes 1–3*, respectively) exhibited a band of 87 kDa as well as a 76-kDa fragment, corresponding to the full-length γ ENaC molecule and the endogenous cleavage product, respectively. In addition, the hNE-treated oocytes exhibited an additional fragment of 67 kDa (Fig. 5*B*, *lane 2*, *) that was not present when oocytes were exposed to hNE in the presence of EPI-hNE4 (*lane 3*). The non-biotinylated protein pool (Fig. 5*C*) similarly contained the 87-kDa full-length γ ENaC molecule, as well as the 76-kDa fragment, but not the 67-kDa fragment in all ENaC-injected conditions (*lanes 1–3*). These products were ENaC specific and not observed in water-injected oocytes (*lane 4*). This result indicated that γ ENaC was cleaved by endogenous proteases and further cleaved by hNE at the cell surface. The corresponding amiloride-sensitive I_{Na} currents are shown in *panel A* showing a 6-fold increase of I_{Na} after 2 min of incubation in the presence of elastase, an effect fully inhibited by the inhibitor.

Western blot densitometry was performed (Molecular Imager FX; Bio-Rad) to quantify the appearance of the hNE-induced 67-kDa γ rENaC fragment at the cell surface (Fig. 6*A*) and in the non-biotinylated total pool (Fig. 6*B*). Band densities of five independent Western blots were normalized to full-length 87-kDa γ ENaC in untreated oocytes (Fig. 6, *A* and *B*, *lanes 1*). Biotinylated cell surface 87-kDa γ ENaC band density was not significantly altered by exposure to hNE alone or when co-incubated with its inhibitor EPI-hNE4 (Fig. 6*A*, *lanes 2* and *3*). Cell surface 76-kDa γ ENaC was similarly not affected (*lanes*

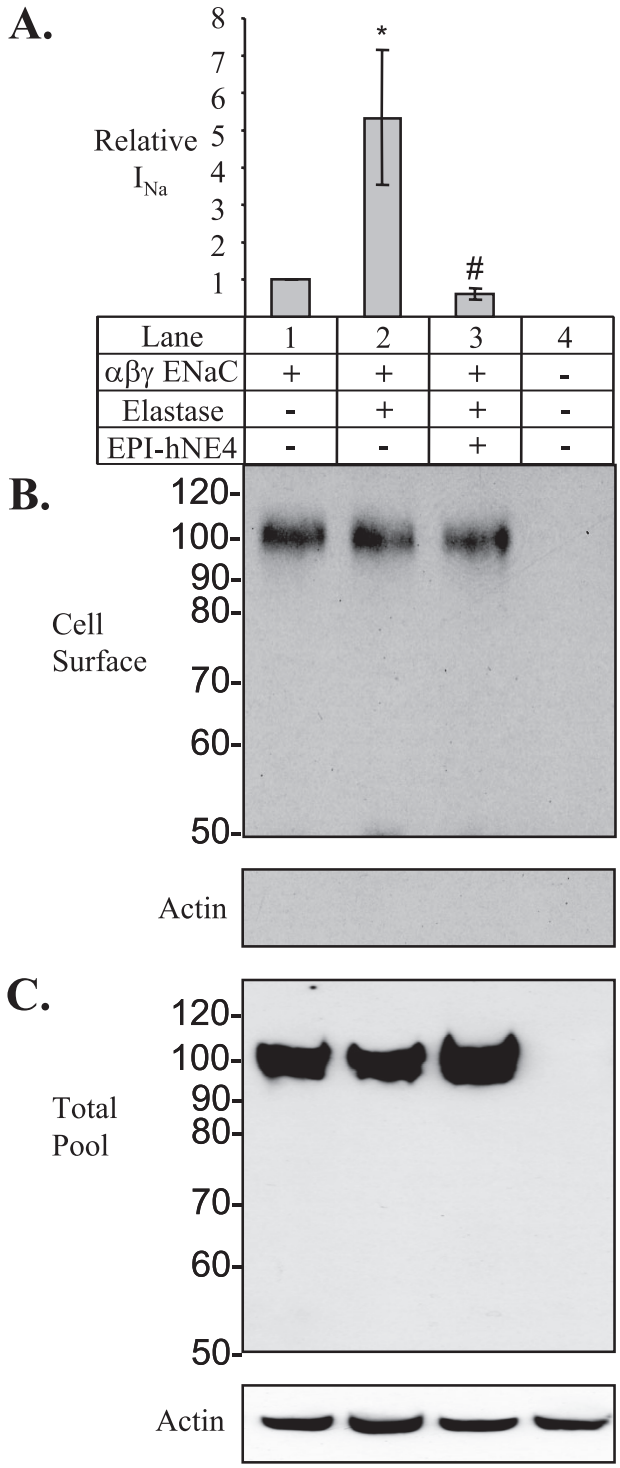

FIGURE 4. **hNE does not cleave cell surface-expressed β ENaC.** Wild-type α and γ rENaC were co-injected with V5-tagged β rENaC in *X. laevis* oocytes. *A*, amiloride-sensitive current was measured in untreated oocytes (2.7 ± 1.3 μA, *lane 1*), oocytes exposed to 10 μg/ml hNE (*lane 2*), 10 μg/ml hNE in the presence of EPI-hNE4 (*lane 3*), and non-injected oocytes (*lane 4*) in five independent experiments. hNE significantly activated ENaC (*, $p < 0.05$), and this activation was inhibited by EPI-hNE4 (#, $p < 0.05$). Cell surface-biotinylated proteins (*surface*) and non-biotinylated proteins (*total pool*) were probed with V5 antibody to detect the V5 tag inserted in the C terminus of β ENaC. *B*, biotinylated cell surface proteins. Full-length 105-kDa β ENaC was expressed at the cell surface in ENaC-injected oocytes (*lanes 1–3*). Treatment with hNE did not produce any additional cleavage products (*lane 2*). *C*, non-biotinylated protein pool. The non-biotinylated protein pool contained the full-length β ENaC in ENaC-injected oocytes (*lanes 1–3*). Absence of actin in the biotinylated proteins indicated that no non-biotinylated proteins were labeled. Even quantities of actin in the non-biotinylated proteins indicated even protein loading.

4–6). The hNE-induced 67-kDa fragment was significantly increased by hNE treatment (*lane 8*, *, $p < 0.05$) over untreated controls (*lane 7*). The appearance of the hNE-induced 67-kDa fragment was prevented by inhibiting hNE with EPI-hNE4 (*lane 8 versus lane 7*, #, $p < 0.05$).

The non-biotinylated total pool 87- and 76-kDa γ rENaC band densities were not significantly affected by treatment with hNE nor hNE with EPI-hNE4 (Fig. 6*B*, *lanes 1–6*). The 67-kDa γ rENaC band was not detected in the non-biotinylated total pool protein (*lanes 7–9*). These results indicated that the hNE-induced 67-kDa γ rENaC cleavage product was significantly increased relative to non-hNE treated controls and that inhibition of hNE by EPI-hNE4 prevented the formation of this cleavage product. The presence of the 67-kDa γ rENaC cleavage product at the cell surface and not in the non-biotinylated total protein pool indicated that hNE was acting uniquely on cell surface-expressed γ rENaC and not on the intracellular γ rENaC proteins.

DISCUSSION

Elastase-induced ENaC Activation and Cleavage at the Cell Surface: Evidence for Specific Exogenous Proteolysis—Recent evidence clearly indicates that ENaC activation can be directly induced by exposing membrane patches to external trypsin (17) or elastase (17). The effect is rapid, characterized by a large change in ENaC open probability (P_o). Obviously, this approach does not allow the correlation of ENaC activity with proteolysis.

In the present study, we took advantage of the very rapid ENaC activation (within 2 min) by external application of hNE, which can then be correlated with the pattern of proteolysis at the cell surface in the same oocytes. A short time course (2 min) minimizes the problem of endo- or exocytosis so that mainly the pool of ENaC molecules pre-existing at the plasma membrane are studied. We used a highly specific elastase inhibitor to definitively assign induced functional and biochemical events to elastase catalytic activity. Using this protocol we have demonstrated that the γ ENaC subunit undergoes a cleavage that is cell surface specific (within 2 min), because it is not observed in the intracellular pool. The induced fragment is 67 kDa, (Fig. 5, *). Cell surface cleavage was efficiently prevented by the elastase inhibitor EPI-hNE4. It is therefore tempting to speculate that this cell surface-specific cleaved form of γ ENaC represents the activation of "near silent" channels observed in membrane patches. In other words, the change in P_o may not only correlate with, but be caused by, proteolysis. How could cleaving a channel increase its P_o? This is not so unlikely if one considers the number of biological processes, *e.g.* prohormones (*i.e.* insulin), the coagulation cascade, that are activated by cleavage. Serine proteases (trypsin, chymotrypsin) secreted as inactive pro-enzymes and activated into zymogens by intramolecular cleavage are other well known examples. A similar scheme could also apply to an ionic channel, such as ENaC. ENaC is characterized by its unusual gating kinetics, with postulated transitions from different modes, *i.e.* from low P_o (*i.e.*"near silent", $P_o < 0.05$) to

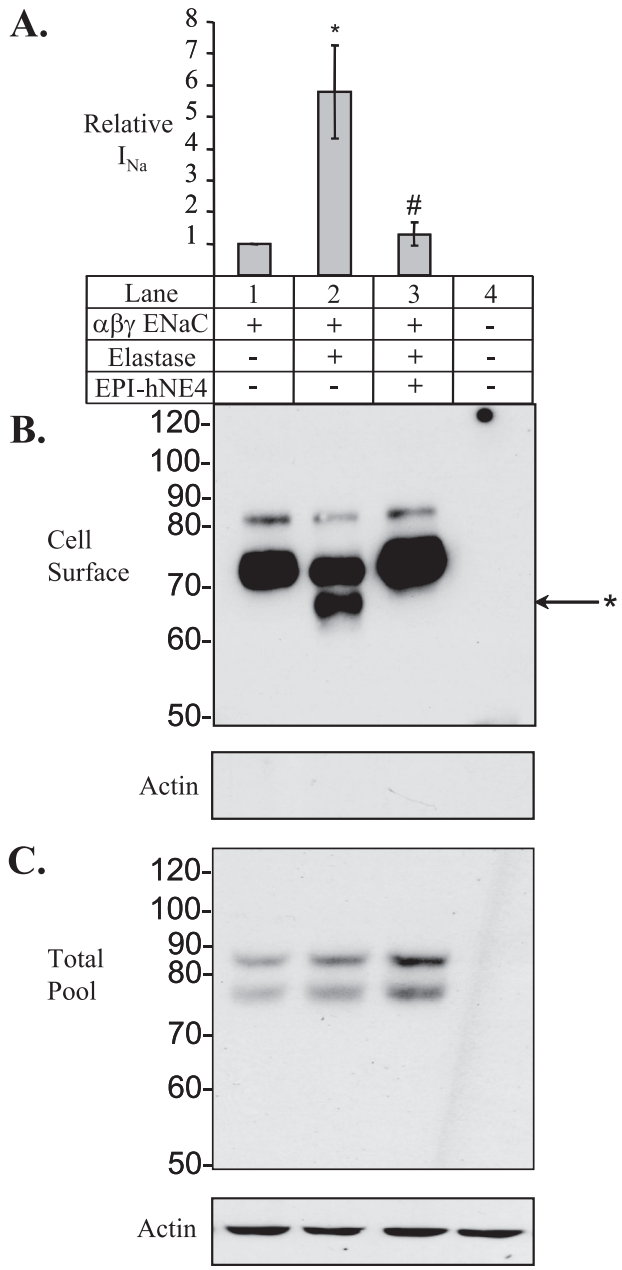

FIGURE 5. **hNE cleaves cell surface-expressed γ ENaC.** Wild-type α and β rENaC were co-injected with V5-tagged γ rENaC in *X. laevis* oocytes. *A*, amiloride-sensitive current was measured in untreated oocytes (3.0 ± 0.9 μA, *lane 1*), oocytes exposed to 10 μg/ml hNE (*lane 2*), 10 μg/ml hNE in the presence of EPI-hNE4 (*lane 3*), and non-injected oocytes (*lane 4*) in five independent experiments. hNE significantly activated ENaC (*, $p < 0.05$), and this activation was inhibited by EPI-hNE4 (#, $p < 0.05$). Cell surface-biotinylated proteins (*surface*) and non-biotinylated proteins (*total pool*) were probed with V5 antibody to detect the V5 tag inserted in the C terminus of γ ENaC (*lanes 1–4*). *B*, biotinylated cell surface proteins. Full-length 87-kDa γ ENaC as well as the 76-kDa fragment were expressed at the cell surface in ENaC-injected oocytes (*lanes 1–3*). Treatment with hNE resulted in an additional γ ENaC cleavage product (*, *lane 2*) relative to the non-treated ENaC-injected oocytes (*lane 1*). The appearance of this additional band was prevented when oocytes were treated with the hNE inhibitor EPI-hNE4 and hNE, simultaneously (*lane 3*). *C*, non-biotinylated protein pool. The non-biotinylated protein pool contained the full-length 87-kDs γ ENaC and the 76-kDa endogenous cleavage product (*lanes 1–3*). Absence of actin in the biotinylated proteins indicated that no intracellular proteins were labeled. Even quantities of actin in the intracellular proteins indicated even protein loading.

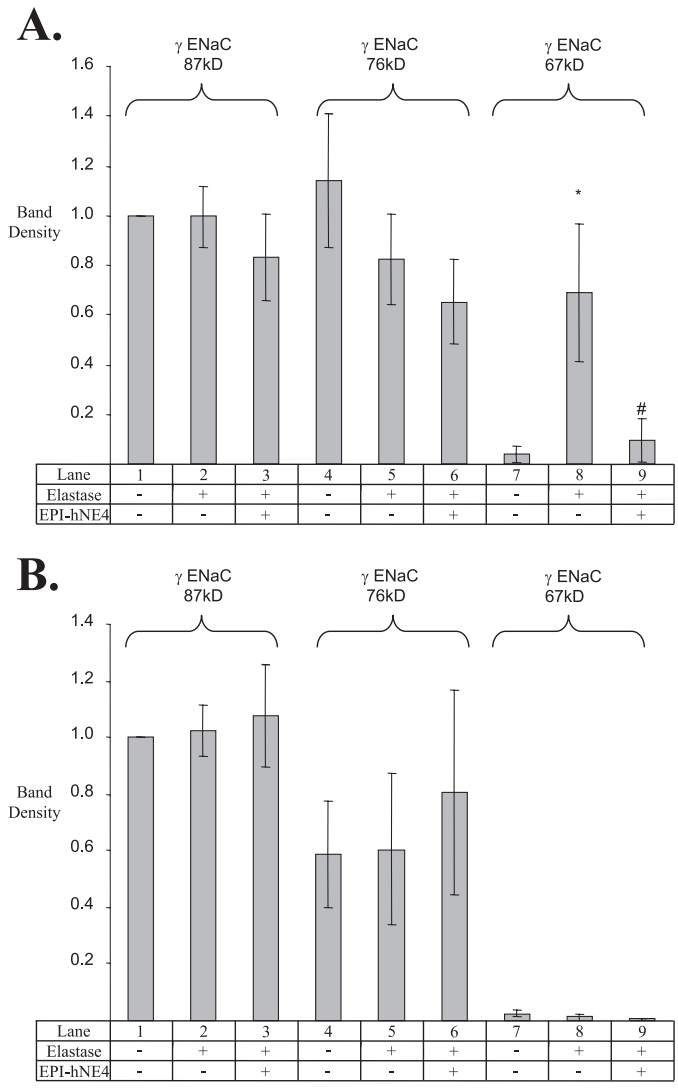

FIGURE 6. **Western blot densitometry of γ ENaC.** Western blots of biotinylated and non-biotinylated V5-tagged γ ENaC were analyzed using a Bio-Rad densitometer in five independent experiments. *A*, cell surface-biotinylated γ ENaC band intensity was normalized to the 87-kDa γ ENaC band in untreated ENaC-injected oocytes (*lane 1*). Neither hNE treatment (*lane 2*) nor treatment with hNE and EPI-hNE4 (*lane 3*) significantly affected the quantity of 87-kDa γ ENaC at the cell surface. The 76-kDa γ ENaC fragment was expressed at the cell surface in ENaC-injected oocytes (4–6). Neither treatment with hNE (*lane 5*) nor with hNE and EPI-hNE4 (*lane 6*) changed the intensity of the 76-kDa γ ENaC fragment significantly. There was a significant increase in the intensity of the 67-kDa γ ENaC fragment when oocytes were treated with hNE (*lane 8*, * denotes $p < 0.05$), but this band was not present in untreated oocytes (*lane 7*) or in oocytes treated with hNE in the presence of EPI-hNE4 (*lane 9*). *B*, non-biotinylated γ ENaC band intensity was normalized to the 87-kDa γ ENaC band in untreated ENaC-injected oocytes (*lane 1*). Neither hNE treatment (*lane 2*) nor treatment with hNE and EPI-hNE4 (*lane 3*) significantly affected the quantity of 87-kDa γ ENaC in the non-biotinylated ENaC-injected oocytes. The endogenously cleaved 76-kDa γ ENaC fragment was present in the non-biotinylated ENaC-injected oocytes (4–6). Neither treatment with hNE (*lane 5*) nor with hNE and EPI-hNE4 (*lane 6*) changed the intensity of the 76-kDa γ ENaC fragment significantly. The 67-kDa γ ENaC band was not present in the non-biotinylated proteins (*lanes 7–9*).

high P_o gating modes ($P_o > 0.8$) (1). These different gating modes could correspond to the cleavage of γ ENaC. Importantly, the β subunit is insensitive to both endogenous and exogenous proteolysis (Fig. 4). We have no explanation for this resistance. One can, however, speculate that the *N*-glycosylation of the β subunit might play a role because the β subunit has

no less than 12 *N*-glycosylation sites. This could protect the proteolytic cleavage sites from enzyme access to their substrate. In addition, it is worth noting that the primary sequence of the β subunit does not have any consensus sequences for cleavage by furin. Therefore, differences in primary sequence and protein folding/maturation may explain the striking difference between the β and γ subunits.

Interestingly, the α ENaC subunit undergoes endogenous cleavage producing an 80-kDa fragment and a 65-kDa fragment at the cell surface (Fig. 3*A*). These cleavage products are not seen in the non-biotinylated intracellular pool (Fig. 3*B*) as an abundant form of the channel. However, overexposure of the Western blot reveals that these fragments are present intracellularly in low quantities relative to the full-length 95-kDa α ENaC (data not shown). Taken together these data indicate that α ENaC is endogenously processed late in its maturation, consistent with a furin cleavage profile, which occurs in the late Golgi or at the cell surface.

Our Western blots of α ENaC indicate that hNE is unable to further cleave this subunit. However, in a small percentage (6%) of our Western blots cleavage of the α ENaC subunit is observed upon exposure to hNE. This is, however, inconsistent with the activation of I_{Na} by hNE that is observed in all experiments irrespective of the hNE-specific cleavage of α ENaC. This is in contrast to the hNE-induced 67-kDa γ ENaC cleavage product that is observed to correlate 100% with induction of I_{Na}.

Physiological and Pathophysiological Implications of Serine Proteases and Serine Protease Inhibitors—Our findings are relevant to the development of novel drug therapies for patients suffering from CF. In this disease, mucociliary clearance is severely decreased. Mucociliary clearance is critically dependent on the control of the periciliar liquid (PCL). Combined defects of accelerated Na^+ transport and the failure to secrete Cl^- deplete the PCL compartment, abrogating both cilia-dependent and cough clearance. Subsequent to PCL depletion, mucus adheres to airway surfaces and persistent mucin secretion generates the formation of "thickened" mucus plaques and plugs, which become the nidus for bacterial infection (10). This pathogenic scheme has been validated by the generation of a mouse model overexpressing the β ENaC subunit in distal airways that led to a PCL depletion and CF lung phenotype mimicking the human disease (11). In this setting, ENaC becomes a valid target for the treatment of CF lung disease. The inhibition of ENaC by amiloride has already been shown to be effective in increasing mucociliary clearance (27). Similar beneficial effects can be observed by inhalation of hypertonic saline, producing a sustained acceleration of mucus clearance and improved lung function (26). Inhibition of elastase by the specific inhibitor would have dual and synergistic effects on CF airways: blocking ENaC activity, thereby repleting PCL and improving mucociliary clearance, and blocking the effect of elastase on tissue inflammation and destruction. This inhibitor would have the advantage of not interfering with the physiological control of ENaC by endogenous lung serine proteases, such as prostasin or other membrane-bound serine proteases, expressed in airway epithelia (15).

REFERENCES

1. Kellenberger, S., and Schild, L. (2002) *Physiol. Rev.* **82,** 735–767
2. Hummler, E., Barker, P., Gatzy, J., Beermann, F., Verdumo, C., Schmidt, A., Boucher, R., and Rossier, B. C. (1996) *Nat. Genet.* **12,** 325–328
3. Boucher, R. C. (2003) *Pflugers. Arch. Eur. J. Physiol.* **445,** 495–498
4. Knowles, M. R., and Boucher, R. C. (2002) *J. Clin. Investig.* **109,** 571–577
5. Rossier, B. C., Pradervand, S., Schild, L., and Hummler, E. (2002) *Annu. Rev. Physiol.* **64,** 877–897
6. Kerem, E., Bistritzer, T., Hanukoglu, A., Hofmann, T., Zhou, Z., Bennett, W., MacLaughlin, E., Barker, P., Nash, M., Quittell, L., Boucher, R., and Knowles, M. R. (1999) *N. Engl. J. Med.* **341,** 156–162
7. Welsh, M. J., and Smith, A. E. (1993) *Cell* **73,** 1251–1254
8. Guggino, W. B. (1999) *Cell* **96,** 607–610
9. Matalon, S., Lazrak, A., Jain, L., and Eaton, D. C. (2002) *J. Appl. Physiol.* **93,** 1852–1859
10. Boucher, R. C. (2004) *Eur. Respir. J.* **23,** 146–158
11. Mall, M., Grubb, B. R., Harkema, J. R., O'Neal, W. K., and Boucher, R. C. (2004) *Nat. Med.* **10,** 487–493
12. Rossier, B. C. (2004) *Proc. Am. Thorac. Soc.* **1,** 4–9
13. Bridges, R. J., Newton, B. B., Pilewski, J. M., Devor, D. C., Poll, C. T., and Hall, R. L. (2001) *Am. J. Physiol.* **281,** L16–L23
14. Tong, Z., Illek, B., Bhagwandin, V. J., Verghese, G. M., and Caughey, G. H. (2004) *Am. J. Physiol.* **287,** L928–L935
15. Planes, C., Leyvraz, C., Uchida, T., Angelova, M. A., Vuagniaux, G., Hummler, E., Matthay, M., Clerici, C., and Rossier, B. (2005) *Am. J. Physiol.* **288,** L1099–L10109
16. Hughey, R. P., Bruns, J. B., Kinlough, C. L., Harkleroad, K. L., Tong, Q., Carattino, M. D., Johnson, J. P., Stockand, J. D., and Kleyman, T. R. (2004) *J. Biol. Chem.* **279,** 18111–18114
17. Caldwell, R. A., Boucher, R. C., and Stutts, M. J. (2004) *Am. J. Physiol.* **286,** C190–C194
18. Konstan, M. W., Hilliard, K. A., Norvell, T. M., and Berger, M. (1994) *Am. J. Respir. Crit. Care Med.* **150,** 448–454
19. Birrer, P., McElvaney, N. G., Rudeberg, A., Sommer, C. W., Liechti-Gallati, S., Kraemer, R., Hubbard, R., and Crystal, R. G. (1994) *Am. J. Respir. Crit. Care Med.* **150,** 207–213
20. Nakamura, H., Yoshimura, K., McElvaney, N. G., and Crystal, R. G. (1992) *J. Clin. Investig.* **89,** 1478–1484
21. Delacourt, C., Herigault, S., Delclaux, C., Poncin, A., Levame, M., Harf, A., Saudubray, F., and Lafuma, C. (2002) *Am. J. Respir. Cell Mol. Biol.* **26,** 290–297
22. Amitani, R., Wilson, R., Rutman, A., Read, R., Ward, C., Burnett, D., Stockley, R. A., and Cole, P. J. (1991) *Am. J. Respir. Cell Mol. Biol.* **4,** 26–32
23. Caldwell, R. A., Boucher, R. C., and Stutts, M. J. (2005) *Am. J. Physiol.* **288,** L813–L819
24. Michlig, S., Harris, M., Loffing, J., Rossier, B. C., and Firsov, D. (2005) *J. Biol. Chem.* **280,** 38264–38270
25. Hughey, R. P., Mueller, G. M., Bruns, J. B., Kinlough, C. L., Poland, P. A., Harkleroad, K. L., Carattino, M. D., and Kleyman, T. R. (2003) *J. Biol. Chem.* **278,** 37073–37082
26. Donaldson, S. H., Bennett, W. D., Zeman, K. L., Knowles, M. R., Tarran, R., and Boucher, R. C. (2006) *N. Engl. J. Med.* **354,** 241–250
27. Sood, N., Bennett, W. D., Zeman, K., Brown, J., Foy, C., Boucher, R. C., and Knowles, M. R. (2003) *Am. J. Resp. Crit. Care Med.* **167,** 158–163